FUNCTIONALLY GRADED PIEZOELECTRIC SMART ACTUATOR DESIGN USING A TOPOLOGY OPTIMIZATION APPROACH

Ronny Calixto Carbonari
ronny@usp.br

César Yukishigue Kiyono
ckiyono@gmail.com

Emílio Carlos Nelli Silva
ecnsilva@usp.br
Department of Mechatronics and Mechanical Systems Engineering,
Escola Politécnica da Universidade de São Paulo,
Av. Prof. Mello Moraes, 2231, 05508-900, São Paulo, SP, Brazil.

Abstract. *Functionally Graded Materials (FGMs) possess continuous variation of material properties and are characterized by spatially varying microstructures. Recently, the FGM concept has been explored in piezoelectric materials to improve properties and to increase the lifetime of piezoelectric actuators. Elastic, piezoelectric, and dielectric properties are graded along the thickness of a piezoceramic FGM. Thus, the gradation of piezoceramic properties can influence the performance of piezoactuators, and an optimum gradation can be sought through optimization techniques. However, the design of these FGM piezoceramics are usually limited to simple configurations. An interesting approach to be investigated is the design of FGM piezoelectric mechanisms, which essentially can be defined as an FGM structure with complex topology made of piezoelectric and non-piezoelectric materials that must generate output displacement and force at a certain specified point of the domain and direction. This can be achieved by means of topology optimization techniques. Thus, in this work, a topology optimization formulation that allows the simultaneous search for an optimal topology of a FGM structure (made of piezoelectric and non-piezoelectric materials) in the design domain, to achieve certain specified actuation movements, will be presented. The optimization problem is posed as the design of the FGM structure that maximizes output displacements or output forces in a certain specified direction and point of the domain. To provide realistic designs, the material gradation is constrained to one-dimension. The method is implemented based on the "Solid Isotropic Material with Penalization" (SIMP) model where fictitious densities are interpolated in each finite element, providing a continuum material distribution in the domain. A gradient control for material gradation was implemented allowing us to analyze the influence of property gradation in the actuator performance. The optimization algorithm employed is based on sequential linear programming (SLP). Two types of FGM piezoelectric mechanisms were designed to demonstrate the usefulness of the proposed method.*

Keywords: *Nanopositioners, MEMS, FGM, Piezoelectric Actuators, Topology Optimization.*

1. INTRODUCTION

Piezoelectric micro-tools offer significant promise in a wide range of applications involving nanopositioning and micromanipulation (Ishihara et al. 1996). For instance, piezoelectric positioners are applied to atomic force microscopes (AFM) and scanning tunneling microscopes (STM) for positioning the sample or the probe, respectively (Indermuhle et al. 1995); piezoelectric micrograppers are applied to micromanipulation (Pérez et al. 2005), cell manipulation and microsurgery (Menciassi et al. 2003). The micro-tools usually consist of multi-flexible structures actuated by two or more functionally graded piezoceramic devices that must generate different output displacements and forces at different specified points of the domain and on different directions. Thus, the development of these piezoelectric micro-tools require the design of actuated compliant mechanisms (Howell 2001) that can perform detailed specific movements. Although the design of such micro-tools is complicated due to the coupling between movements generated by various piezoceramics, it can be realized by means of topology optimization (Canfield and Frecker 2000; Carbonari et al. 2005) which even allows the simultaneous search for an optimal topology of a flexible structure as well as the optimal positions of the piezoceramics in the design domain, to achieve certain specified actuation movements (Carbonari et al. 2007).

Functionally Graded Materials (FGMs) are special materials that possess continuously graded properties and are characterized by spatially varying microstructures created by nonuniform distributions of the reinforcement phase as well as by interchanging the role of reinforcement and matrix (base) materials in a continuous manner (Miyamoto et al. 1999). The smooth variation of properties may offer advantages such as local reduction of stress concentration and increased bonding strength.

Topology optimization is a powerful structural optimization method that seeks an optimal structural topology design by determining which points of space should be solid and which points should be void (i.e. no material) inside a given

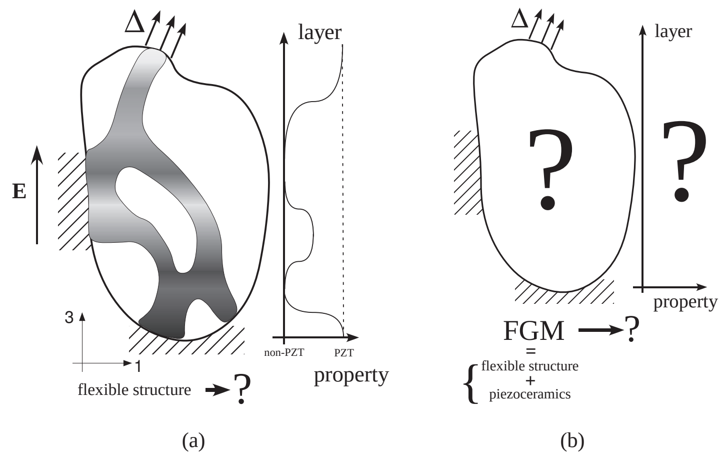

Figure 1. (a) Conventional FGM piezoactuator design (FGM piezoceramic position is fixed); (b) FGM piezoelectric device design considering the simultaneous distribution of FGM piezoceramic and void in the design domain.

domain (Bendsøe and Sigmund 2003). However, the binary $(0-1)$ design is an ill-posed problem and a typical way to seek a solution for topology optimization problems is to relax the problem by defining a material model that allows for intermediate (composites) property values. In this sense, the relaxation yields a continuous material design problem that no longer involves a discernible connectivity. Typically, it is an improperly formulated (ill-posed) topology optimization problem for which no optimum solution exists (0-1 design). A topology solution can be obtained by applying penalization coefficients to the material model to recover the 0-1 design (and thus, a discernible connectivity), and some gradient control of material distribution, such as a filter for example (Bendsøe and Sigmund 2003; Belytschko et al. 2003).

The relaxed problem is strongly related to the functionally graded material (FGM) design problem, which essentially seeks a continuous transition of material properties (Miyamoto et al. 1999). In contrast, while the $0-1$ design problem does not admit intermediate values of design variables, the FGM design problem does admit solutions with intermediate values of the material field.

Due to the attractive possibilities of tailoring the material properties, some researchers have applied optimization methods to design FGMs (Turteltaub 2002b). The application of a generic optimization method to tailor material property gradation has been proposed by Paulino and Silva (Paulino and Silva 2005) who applied topology optimization to solve the problem of maximum stiffness design.

Recently, the concept of functionally graded materials (FGMs) has been explored in piezoelectric materials to improve their properties and increase the lifetime of piezoelectric actuators (Almajid et al. 2001). Usually, elastic, piezoelectric, and dielectric properties are graded along the thickness of an FGM piezoceramic. Previous studies (Almajid et al. 2001; Zhifei 2002) have shown that the gradation of piezoceramic properties can influence the performance of piezoactuators, such as generated output displacements. This suggests that optimization techniques can be applied to take advantage of the property gradation variation to improve the FGM piezoactuator performance.

However, the design of these FGM piezoactuators are usually limited to simple shapes. An interesting approach to be investigated is to mix the concept of FGM with micro-tools, that is, to design FGM piezoelectric mechanisms which essentially can be defined as a FGM structure with complex topology made of piezoelectric and non-piezoelectric material that must generate output displacement and force at a certain specified point of the domain and direction. This can be achieved by using topology optimization method.

Thus, the objective of this work is to develop a topology optimization formulation that allows the simultaneous distribution of void and FGM piezoelectric material (made of piezoelectric and non-piezoelectric material) in the design domain, to achieve certain specified actuation movements. Two design problems are considered simultaneously: the optimum design of the piezoceramic property gradation in the FGM piezoceramic domain,and the design of the FGM structural topology. Figure 1 illustrates the concept of FGM piezoelectric devices proposed in this work.

The optimization problem is posed as the design of a FGM structure, as well as its property gradation that maximizes output displacement or output force in a specified direction and point of the domain, while minimizing the effects of movement coupling (Carbonari et al. 2005). The method is implemented based on the solid isotropic material with penalization (SIMP) model where fictitious densities are interpolated at each finite element, providing a continuous material distribution in the domain. The optimization algorithm employed is based on sequential linear programming (SLP) (Vanderplaatz 1984; Hanson and Hiebert 1981). Since the position of piezoceramic are not known Şa prioriŤ an independent electrical excitation is considered for each finite element which is equivalent to a constant applied electric field (Carbonari et al. 2007). This decouples the electrical and mechanical problem, however, the dielectric properties are not taken into account in the design problem.

Thus, this formulation contributes to increase the design flexibility of these devices allowing the design of novel types of FGM piezoactuators for different applications. Two FGM piezoelectric mechanisms were designed to demonstrate the usefulness of the proposed method. An one-dimensional constraint of the FGM gradation is imposed to provide more realistic designs. The use of topology optimization for the design of FGM piezoactuators is a novel approach that has the potential to dramatically broaden the applied range of such devices, especially in the field of smart structures.

2. Finite Element FGM Piezoelectric Modeling

The micro-tools considered here operate in quasi-static or low-frequency modes (inertia effects are neglected). When a non-piezoelectric conductor material and a piezoceramic material are distributed in the piezoceramic domain, the electrode positions are not known "a priori", as discussed ahead. Thus, the electrical excitation is given by an applied electric field (Carbonari et al. 2007) ($\nabla\phi$=constant). In this case, all electrical degrees of freedom are specified in the FE problem, and thus the linear finite element (FE) matrix formulation of the equilibrium equations for the piezoelectric medium is given by (Lerch 1990):

$$\begin{bmatrix} \mathbf{K}_{uu} & \mathbf{K}_{u\phi} \\ \mathbf{K}_{u\phi}^{t} & -\mathbf{K}_{\phi\phi} \end{bmatrix} \begin{Bmatrix} \mathbf{U} \\ \mathbf{\Phi} \end{Bmatrix} = \begin{Bmatrix} \mathbf{F} \\ \mathbf{Q} \end{Bmatrix} \Longrightarrow [\mathcal{K}]\{\mathcal{U}\} = \{\mathcal{Q}\} \tag{1}$$

where $\mathbf{K}_{uu}$, $\mathbf{K}_{u\phi}$, and $\mathbf{K}_{\phi\phi}$ denote the stiffness, piezoelectric, and dielectric matrices, respectively, and $\mathbf{F}$, $\mathbf{Q}$, $\mathbf{U}$, and $\mathbf{\Phi}$ are the nodal mechanical force, nodal electrical charge, nodal displacements, and nodal electric potential vectors, respectively (Lerch 1990).

In the case of FGM piezoceramics, the properties change continuously inside the piezoceramic domain, which means that they can be described by some continuous function of position $\mathbf{x}$ in the piezoceramic domain, that is:

$$\mathbf{C} = \mathbf{C}(\mathbf{x})\,; \quad \mathbf{e} = \mathbf{e}(\mathbf{x})\,; \quad \boldsymbol{\epsilon}^{S} = \boldsymbol{\epsilon}^{S}(\mathbf{x}) \tag{2}$$

From the mathematical definitions of $\mathbf{K_{uu}}$, $\mathbf{K_{u\phi}}$, and $\mathbf{K}_{\phi\phi}$, these material properties must remain inside the matrices integrals and be integrated together by using the graded finite element concept (Kim and Paulino 2002) where properties are continuously interpolated inside each finite element based on property values at each finite element node. An attempt to approximate the continuous change of material properties by a stepwise function where a property value is assigned for each finite element may result in less accurate results with undesirable discontinuities of the stress and strain fields. Therefore, the mechanical and electrical problems are decoupled, and only the upper problem of Eq. 1 needs to be directly solved. Essentially, the optimization problem is based on the mechanical problem. As a consequence, the dielectric properties do not influence the design.

3. Design Problem Formulation

For topology optimization (Carbonari et al. 2005) numerical implementation, we are considering the continuous distribution of the design variable inside the finite element by interpolating it using the FE shape functions. In this case, the design variables are defined for each element node. We are interested in a simultaneous distribution of void, and FGM piezoelectric material in the design domain, and thus, the following material model is proposed based on an simple extension of the SIMP ("Solid Isotropic Material with Penalization") model (Carbonari et al. 2007):

$$\mathbf{C} = \rho_1^{p_{c1}}\left[\rho_2\mathbf{C}_1 + (1-\rho_2)\,\mathbf{C}_2\right] + \left(1-\rho_1^{p_{c1}}\right)\mathbf{C}_{\text{void}} \tag{3}$$

$$\mathbf{e} = \rho_1^{p_{c1}}\left[\rho_2\mathbf{e}_1 + (1-\rho_2)\,\mathbf{e}_2\right], \tag{4}$$

where ρ_1 and ρ_2 are pseudo-density function representing the amount of material at each point of the domain. These pseudo-densities can assume different values at each finite element node. Thus, ρ_1 = 1.0 denotes FGM material and ρ_1 = 0.0 denotes void, and ρ_2 = 1.0 denotes piezoelectric material **type** 1 or ρ_1 = 0.0 denotes piezoelectric material **type** 2. **C** and **e** are stiffness and piezoelectric tensor properties, respectively, of the material. The tensors $\mathbf{C}_j$ and $\mathbf{e}_j$ are related to the stiffness and piezoelectric properties for piezoelectric material type j (j = 1, 2), respectively. $\mathbf{C}_{void}$ is the tensor related to void stiffness property. Eventually, the piezoelectric material **type** 2 can be substituted by the flexible structure material (non-piezoelectric material, such as Aluminum, for example), and in this case $\mathbf{e}_2 = 0$. These are the properties of basic materials that are distributed in the piezoceramic domain. The dielectric properties are not considered because a constant electric field is applied to the design domain as electrical excitation, this approach decouples the electrical and mechanical problems eliminating the influence of dielectric properties in the optimization problem. $pc1$ is a penalization factor to recover the discrete design, and its value varies from 0 to 3. For a discretized domain into finite elements, Eq. 3 and 4 are considered for each element node, and the material properties inside each finite element are given by functions of x (($\rho_1(\mathbf{x})$ and ($\rho 2(\mathbf{x})$). This formulation leads to a continuous distribution of material along the design domain. Thus, by finding the nodal values of the unknown $\rho_1(\mathbf{x})$ and ($\rho 2(\mathbf{x})$ function, we are indirectly finding the optimum material distribution functions, which are described by Eq. 2.

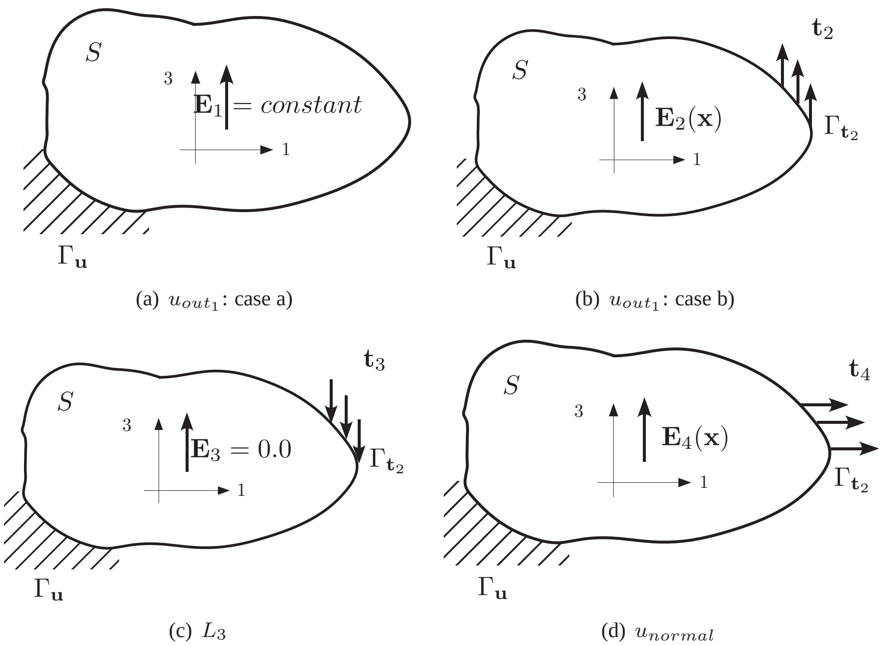

Figure 2. Load cases for calculation of: generated output displacement, mean compliance and generated normal displacement. Here, $\mathbf{E}_i = -\nabla\phi_i$ denotes the electrical field associated with load case i.

In this work, the piezoceramic electrodes are not known "a priori", and, thus, an electric field is applied as electrical excitation. Essentially, the objective function is defined in terms of generated output displacements for a certain applied electric field to the design domain. Considering d_i and $\boldsymbol{\phi}_i$ the electrical displacement and electrical potential related to load case i, respectively, the generated output displacement is defined by (in this work, $\mathbf{E}_1$ is prescribed) (Carbonari et al. 2007):

$$u_{out_1} = \int_{\Gamma_{t_2}} \mathbf{t}_2 \mathbf{u}_1 \, d\Gamma + \int_{\Gamma_{d_2}} d_2 \boldsymbol{\phi}_1 \, d\Gamma = \int_{\Gamma_{t_2}} \mathbf{t}_2 \mathbf{u}_1 \, d\Gamma \tag{5}$$

as $d_2 = 0$ in this problem. The load cases considered for calculation of generated output displacement are shown in instances 2(a) and 2(b) of Figure 2.

However, the optimum solution obtained considering only the maximization of generated output displacement may be a structure with very low stiffness. The piezoactuator must resist to reaction forces (in region $\Gamma_{\mathbf{t}_2}$) generated by a body that the piezoactuator is trying to move or grab. Therefore, the mean compliance must be minimized to provide enough stiffness (see Figure 2(c)). The mean compliance is calculated by considering the load case described in case 2(c) of Figure 2 where a traction $\mathbf{t}_3 = -\mathbf{t}_2$ is applied to region $\Gamma_{\mathbf{t}_2}$ and the electric field is kept null inside the medium ($\mathbf{E}_3 = 0$). The displacement coupling constraint is obtained by minimizing the absolute value of the corresponding undesired generated displacement that is, a displacement normal to the desired displacement, which is calculated by using Eq. 5, however, considering a load case described in case 2(d) of Figure 2 instead, where a traction $\mathbf{t}_4$, normal to $\mathbf{t}_2$, is applied to region $\Gamma_{\mathbf{t}_2}$ (Carbonari et al. 2007).

To properly combine the desired output displacement maximization, mean compliance maximization, and coupling constraint minimization, a multi-objective function is constructed to find an appropriate optimal solution that can incorporate all design requirements. The following multi-objective function is proposed to combine all these optimization aspects (Carbonari et al. 2007):

$$\mathcal{F}(\rho_1, \rho_2) = w * \ln\left[u_{out_1}\right] - \frac{1}{2}(1-w)\ln\left[L_3(\mathbf{u}_3, \boldsymbol{\phi}_3)^2 + \beta\, u_{normal}^2\right], \tag{6}$$

where w is a weight coefficient ($0 \leq w \leq 1$). The coefficient w allows control of the contributions of generated output displacement, mean compliance, and displacement coupling in the design. Accordingly, the final optimization problem is defined as:

$$\begin{array}{ll} \text{Maximize:} & \mathcal{F}(\rho_1, \rho_2) \\ \rho_1(\mathbf{x}), \rho_2(\mathbf{x}) & \\ \text{subject to:} & \text{Equilibrium equations for different load cases} \\ & 0 \leq \rho_1 \leq 1;\ 0 \leq \rho_2 \leq 1; \\ & \Theta_1(\rho) = \int_S \rho_1 dS - \Theta_{1S} \leq 0;\ \Theta_2(\rho) = \int_S \rho_2 dS - \Theta_{2S} \leq 0 \end{array} \tag{7}$$

Here S denotes the design domain, Θ_1 is the volume of this design domain, and Θ_{1S} is an upper-bound volume constraint defined to limit the maximum amount of material used to build the FGM coupling structure. Moreover, Θ_2 is the volume related to ρ_2, and Θ_{2S} is an upper-bound volume constraint defined to limit ρ_2 values when optimizing the FGM gradation function. The other constraints are equilibrium equations for the piezoelectric medium considering different load cases. The equilibrium equations are solved separately from the optimization problem. They are stated in the problem to indicate that, whatever topology is obtained, it must satisfy the equilibrium equations.

4. Numerical Implementation

The continuum distribution of pseudo-densities $\rho_1(\mathbf{x})$ and $\rho_2(\mathbf{x})$ are given by the functions

$$\rho_1(\mathbf{x}) = \sum_{I=1}^{n_d} \rho_{1I} N_I(\mathbf{x}); \quad \boldsymbol{\rho}_2(\mathbf{x}) = \sum_{I=1}^{n_d} \rho_{2I} N_I(\mathbf{x}), \tag{8}$$

where ρ_{1I} and ρ_{2I} are nodal pseudo-densities, N_I is the finite element shape function that must be selected to provide non-negative values of the design variables, and n_d is the number of nodes at each finite element. The pseudo-densities ρ_{1I} and ρ_{2I} can assume different values at each node of the finite element.

Due to the definition of Eq. 8, the material property functions (Eqs. 3 and 4) also have a continuum distribution inside the design domain. Thus, considering the mathematical definitions of the stiffness and piezoelectric matrices of Eq. 1, the material properties must remain inside the integrals and be integrated together by means of the graded finite element concept (Kim and Paulino 2002). The finite element equilibrium Eq. 1 is solved considering 4-node isoparametric finite elements under either plane stress or plane strain assumptions.

When a non-piezoelectric conductor material (usually a metal, such as Aluminum) is considered in Eqs. 3 and 4, a relevant problem to be solved is how to define the piezoceramic electrodes. If a non-piezoelectric conductor material (for example, Aluminum) is distributed in the piezoceramic design domain, we cannot define “a priori” the position of the piezoceramic electrodes because we do not know where the piezoceramic is located in the design domain. To circumvent this problem, we consider the electrical problem independently for each finite element of the piezoceramic domain by defining a pair of electrodes at each finite element, that is, each finite element has its own electrical degrees of freedom.

Thus, each finite element has 4 electrical degrees of freedom given by $[\phi_a, \phi_b, \phi_c, \phi_d]$ (nodes are ordered counter-clockwise starting from the upper right corner of each finite element) considering that one of the electrodes is grounded. Electrical voltage ϕ_0 is applied to the two upper nodes, and thus, the four electrical degrees of freedom are prescribed at each finite element, as follows ($[\phi_0, \phi_0, 0, 0]$) (Carbonari et al. 2007). This is equivalent to applying a constant electrical field along the 3-direction in the design domain. In this case, all electrical degrees of freedom are prescribed in the FE problem. By means of the FE matrix formulation of equilibrium, Eq. 1, the discretized form of the optimization problem given by Eq. 7 is restated as:

$$\begin{array}{lll}
\underset{\rho_{1I},\,\rho_{2I}}{\text{Maximize:}} & \mathcal{F}(\rho_{1I}, \rho_{2I}) & \\
\text{subject to:} & \{\mathbf{F}_3\} = -\{\mathbf{F}_2\} \quad (\Gamma_{\mathbf{t}_3} = \Gamma_{\mathbf{t}_2}) & \\
& \{\mathbf{F}_4\}^t \{\mathbf{F}_2\} = 0 \quad (\Gamma_{\mathbf{t}_4} = \Gamma_{\mathbf{t}_2}) & \\
& [\mathcal{K}_1]\{\mathcal{U}_1\} = \{\mathcal{Q}_1\} & [\mathcal{K}_2]\{\mathcal{U}_2\} = \{\mathcal{Q}_2\} \\
& [\mathcal{K}_3]\{\mathcal{U}_3\} = \{\mathcal{Q}_3\} & [\mathcal{K}_2]\{\mathcal{U}_4\} = \{\mathcal{Q}_4\} \\
& 0 \le \rho_{1I} \le 1; 0 \le \rho_{2I} \le 1 & I = 1..N_e \\
& \sum_{I=1}^{NE} \int_{S_I} \rho_1 dS_I - \Theta_{1S} \le 0 & \\
& \sum_{J=1}^{NE} \int_{S_J} \rho_2 dS_J - \Theta_{2S} \le 0 &
\end{array} \tag{9}$$

where the integrals in the volume constraint expressions are evaluated by using Gauss quadrature (4 points) and considering Eq. 1. The parameter N_e is the number of nodes in the design design domain. Moreover, NE denotes the number of elements in the design domain. The matrices $[\mathcal{K}_1]$ and $[\mathcal{K}_3]$ are reduced forms of the matrix $[\mathcal{K}_2]$ considering non-zero and zero specified voltage degrees of freedom (applied electric field) at the piezoceramic domain, respectively. The initial domain is discretized by finite elements and the pseudo-densities ($\rho_1$and ρ_2) are the values of ρ_{1I} and ρ_{2J} are defined at each finite element node in the design domain.

5. Material Gradation Control

CAMD approach ensures the continuous material distribution across elements. However, it does not provide a general control of the gradient of material distribution. To achieve a meshindependent control of the gradient of material distribution, we introduce a new layer of design variables and use a projection function to obtain the material densities at nodes. This concept of using nodal design variables and projection functions has been developed in (Guest, Prevost, and Belytschko 2004). This concept will be applied on top of the CAMD in this paper.

Let d_{1n} and d_{2n} denote all design variables associated with nodes ρ_{1I} and layers ρ_{2J}, respectively. Assume that the required change of material density must occur over a minimum length of r_{min}. ρ_{1I} and ρ_{2J} can be obtained from d_n using a projection function defined by Guest et al. (2004), as follows:

$$\rho_n = f(d_n), \tag{10}$$

where *f* is the projection function defined as follows.

$$\rho_i = f(d_j) = \frac{\sum_{j\in S_j} d_j w(x_j - x_i)}{\sum_{j\in S_j} w(x_j - x_i)}, \tag{11}$$

and S_i is the set of nodes in the domain of influence of node *i* (Ω_l), which consists in a circle of radius r_{min} and center at node *i*. The weight function *w* is defined as follows.

$$w\left(x_j - x_i\right) = \begin{cases} \frac{r_{min}-r_{ij}}{r_{min}} & \text{if } x_j \in \Omega_l \\ 0 & \text{otherwise} \end{cases}, \tag{12}$$

r_{ij} is the distance between nodes *j* and *i*

$$r_{ij} = \|x_j - x_i\|. \tag{13}$$

The topology optimization problem definition is revised as follows.

$$\begin{array}{lll}
\text{Maximize:} & \mathcal{F}\left(d_n\right) & \\
d_n & & \\
\text{subject to:} & \{\mathbf{F}_3\} = -\{\mathbf{F}_2\} \quad (\Gamma_{\mathbf{t}_3} = \Gamma_{\mathbf{t}_2}) & \\
& \{\mathbf{F}_4\}^t\{\mathbf{F}_2\} = 0 \quad (\Gamma_{\mathbf{t}_4} = \Gamma_{\mathbf{t}_2}) & \\
& [\mathcal{K}_1]\{\mathcal{U}_1\} = \{\mathcal{Q}_1\} & [\mathcal{K}_2]\{\mathcal{U}_2\} = \{\mathcal{Q}_2\} \\
& [\mathcal{K}_3]\{\mathcal{U}_3\} = \{\mathcal{Q}_3\} & [\mathcal{K}_2]\{\mathcal{U}_4\} = \{\mathcal{Q}_4\} \\
& \sum_{I=1}^{NE}\int_{S_I} d_{1n} dS_I - \Theta_{1S} \le 0 & \\
& \sum_{J=1}^{NE}\int_{S_J} d_{2n} dS_J - \Theta_{2S} \le 0 & \\
& 0 \le d_{1n} \le 1; & \\
& 0 \le d_{2n} \le 1; &
\end{array} \tag{14}$$

The mathematical programming method called Sequential Linear Programming (SLP) is applied to solve the optimization problem (Hanson and Hiebert 1981; Vanderplaatz 1984). The linearization of the problem at each iteration requires the sensitivities (gradients) of the multi-objective function and constraints in relation to d_n.

A flow chart of the optimization algorithm describing the steps involved is shown in Figure 3. The software was implemented using the C language.

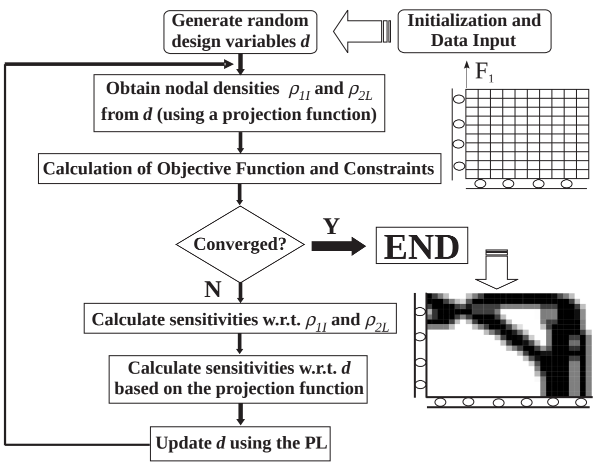

Figure 3. Flow chart of optimization procedure (LP means linear programming).

Suitable moving limits are introduced to assure that the design variables do not change by more than 5–15% between consecutive iterations. A new set of design variables d_n are obtained after each iteration, and the optimization continues until convergence is achieved for the objective function.

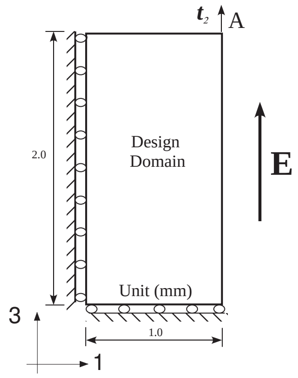

Figure 4. Design domain and load conditions.

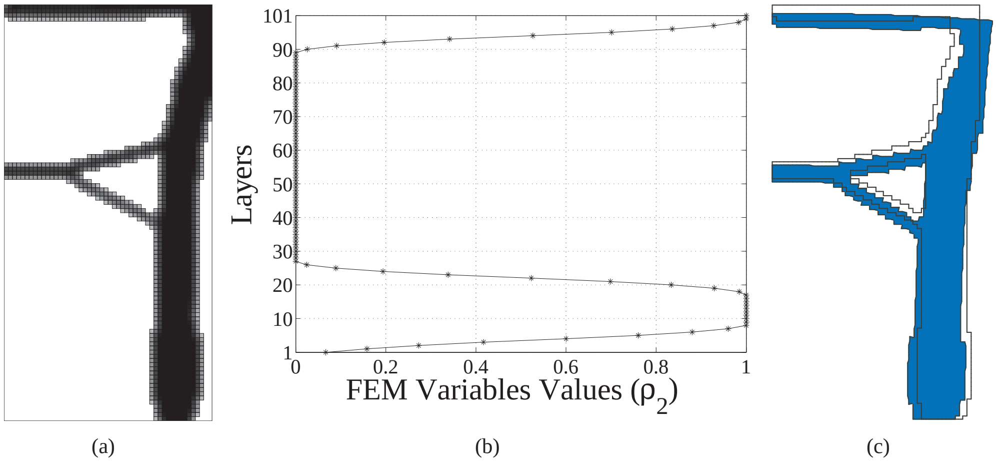

Figure 5. Result for $w = 0.5$, $\beta = 0.0$, $r_{\rho_1} = 0.04mm$ and $r_{\rho_2} = 0.1mm$; a) Optimal topology; b) Material gradation along 3 direction; c) Deformed configuration of interpreted topology.

6. Numerical Results

Examples are presented to illustrate the design piezoelectric actuators using the proposed method. Once the idea is to simultaneously distribute void, and FGM piezoelectric no regions with predefined materials are specified in the design domain S. For all examples, the FGM piezoelectric is composed of piezoelectric material (Carbonari et al. 2005) and Aluminum, and the material gradation is constrained to the 3 direction. $\mathbf{C}$ and $\mathbf{e}$ are the elastic and piezoelectric properties, respectively, of the medium. The Young's modulus and Poisson's ratio of Aluminum are equal to $70\ GPa$ and 0.33, respectively. Two-dimensional isoparametric finite elements under plane-stress assumption are used in the finite element analysis.

The amount of electric field applied to the design domain is 500 V/mm (see Figure 4). The design domain for all examples is shown in Figure 4 which was discretized into 5000 finite elements. The mechanical and electrical boundary conditions are shown in the same figure. The FGM volume constraint and piezoelectric material volume constraint in the FGM are both equal to 25%. The initial values of pseudo-densities ρ_{1I} and ρ_{2I} are equal to 0.15, and the optimization problem starts in the feasible domain (all constraints satisfied). The results are shown by plotting the average density value. The final actuator configuration for all results is obtained by interpreting FGM topology by doing a simple threshold of pseudo-density value ρ_{1I}.

The topology optimization problem was solved considering $w = 0.5$. The β coefficient was set equal to 0.0 and 0.0001 which means that the coupling constraint is not considered in the first case, and it is considered in the second case, respectively. The obtained piezoelectric FGM topologies are shown in Figures 5(a) and 6(a), respectively. The material gradation in the FGM domain along the 3 direction are shown in graphics of Figures 5(b) and 6(b), respectively. Again, a clear contrast among piezoelectric FGM topology and void could be obtained in both cases. The corresponding deformed configuration of interpreted topologies (considering 500 V/mm) are shown in Figures 5(c) and 6(c), respectively. For β equal to 0.0 the piezoceramic is distributed in the upper and lower parts of the design domain, like in the previous example. However, for β equal to 0.0001 the piezoceramic is distributed in lower part. Table 1 describes vertical displacement at point A (see Figure 4) considering $500V/mm$ applied to the piezoceramic finite elements, and the coupling factor R_{xy} which is the ratio between undesired (horizontal) and desired (vertical) displacement. For the second case, a smaller

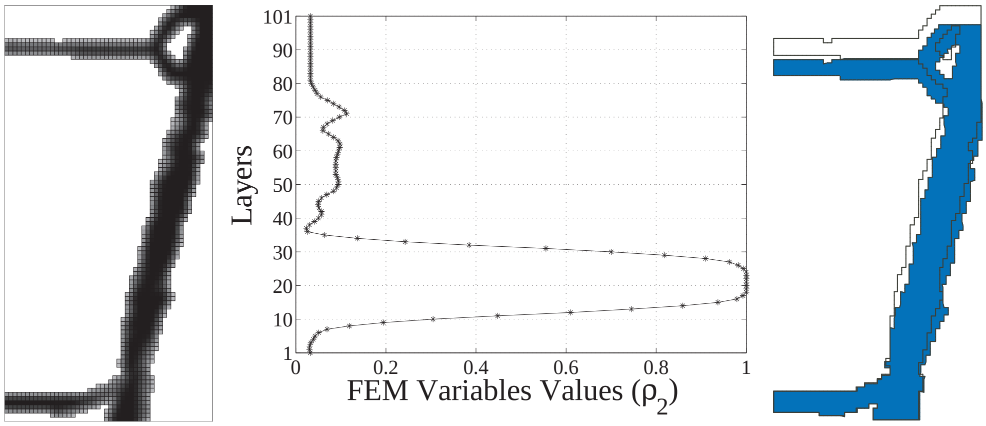

(a) (b) (c)

Figure 6. Result for $w = 0.5$, $\beta = 0.0001$, $r_{\rho_1} = 0.04mm$ and $r_{\rho_2} = 0.1mm$; a) Optimal topology; b) Material gradation along 3 direction; c) Deformed configuration of interpreted topology.

Table 1. Vertical displacement at point A (500 V/mm applied) and coupling factor (R_{yx}).

Piezoactuator	$u_y(\mu m)$	$u_x(\mu m)$	$R_{yx}(\%)$	w	β
Figure 5(c)	1.050	0.859	81.81	0.5	0.0
Figure 6(c)	0.819	0.003	0.37	0.5	10^{-4}

displacement was obtained due to lower value of w (0.5), however, for β equal to 0.0001 a negligible coupling was achieved.

7. Conclusions

A topology optimization formulation was proposed which allows the search of an optimal topology of a FGM piezoelectric structure for designing piezoelectric actuators, to achieve certain specified actuation movements. This is achieved by the optimization problem by allowing the simultaneous distribution of void and FGM piezoelectric in the design domain and applying an electric field as electrical excitation. The composition of FGM piezoelectric may include non-piezoelectric material. The adopted material model in the formulation is based on the density method and it interpolates fictitious densities at each finite element based on pseudo-densities defined as design variables for each finite element node providing a continuous material distribution in the domain. Some 2D examples were presented to illustrate the potentiality of the method. By controlling topology and material gradation large displacement and low displacement coupling constraint can be obtained.

In future work, the designed piezoelectric actuators will be manufactured in a mesoscale by using a spark plasma sintering (SPS) machine, and displacement measurements will be conducted to verify the performance of these designs.

8. Acknowledgements

The first author thanks CNPq (Conselho Nacional de Desenvolvimento Científico e Tecnológico - Brazil), for supporting him through a doctoral fellowship (n.o140687/2003-3). The second author thanks FAPESP (Fundação de Amparo à Pesquisa do Estado de São Paulo - project n.o05/57810- 8). The last author thanks FAPESP (project n.o06/57805- 7), CNPq, and the University of Illinois at Urbana-Champaign (UIUC) for inviting him as a Visiting Professor during the Summer/2006. We gratefully acknowledge the USA NSF through the project CMS0303492 (Inter-Americas Collaboration in Materials Research and Education, PI Prof. W. Soboyejo, Princeton University).

9. REFERENCES

Almajid, A., M. Taya, and S. Hudnut (2001). Analysis of out-of-plane displacement and stress field in a piezocomposite plate with functionally graded microstructure. *International Journal of Solids and Structures 38*(19), 3377–3391.

Belytschko, T., S. P. Xiao, and C. Parimi (2003, June). Topology optimization with implicit functions and regularization. *International Journal for Numerical Methods in Engineering 57*(8), 1177–1196.

Bendsøe, M. P. and O. Sigmund (2003). *Topology Optimization - Theory, Methods and Applications*. New York, EUA: Springer.

Canfield, S. and M. Frecker (2000). Topology optimization of compliant mechanical amplifiers for piezoelectric actuators. *Structural and Multidisciplinary Optimization 20*, 269–279.

Carbonari, R. C., E. C. N. Silva, and S. Nishiwaki (2005). Design of piezoelectric multiactuated microtools using topology optimization. *Smart Materials and Structures 14*, 1431–1447.

Carbonari, R. C., E. C. N. Silva, and S. Nishiwaki (2007). Optimum placement of piezoelectric material in the piezoactuator design. *Smart Materials and Structures 16*(1), 207–220.

Guest, J. K., J. H. Prevost, and T. Belytschko (2004, September). Achieving minimum length scale in topology optimization using nodal design variables and projection functions. *International Journal for Numerical Methods in Engineering 61*(2), 238–254.

Hanson, R. and K. Hiebert (1981). *A Sparse Linear Programming Subprogram*. Technical Report SAND81-0297: Sandia National Laboratories.

Howell, L. L. (2001). *Compliant Mechanisms*. New York, USA: John Wiley & Sons, Inc.

Indermuhle, P., V. Jaecklin, J. Brugger, C. Linder, N. Rooij, and M. Binggeli (1995). Afm imaging with an xy – micropositioner with integrated tip. *Sensors and Actuators A: Physical 47*(1–3), 562–565.

Ishihara, H., F. Arai, and T. Fukuda (1996). Micro mechatronics and micro actuators. *IEEE/ASME Transactions on Mechatronics 1*(1), 68–79.

Kim, J. H. and G. H. Paulino (2002). Isoparametric graded finite elements for nonhomogeneous isotropic and orthotropic materials. *ASME Journal of Applied Mechanics 69*(4), 502–514.

Kögl, M. and E. C. N. Silva (2005). Topology optimization of smart structures: Design of piezoelectric plate and shell actuators. *Journal of Smart Materials and Structures 14*(2), 387–399.

Ku, S., U. Pinsopon, S. Cetinkunt, and S. Nakajima (2000). Design, fabrication, and real-time neural network control of a three-degrees-of-freedom nanopositioner. *IEEE/ASME Transactions on Mechatronics 5*(3), 273–279.

Lerch, R. (1990). Simulation of piezoelectric devices by two-and three-dimensional finite elements. *IEEE Transactions on Ultrasonics, Ferroelectrics and Frequency Control 37*(2), 233–247.

Matsui, K. and K. Terada (2004). Continuous approximation of material distribution for topology optimization. *International Journal for Numerical Methods in Engineering 59*(14), 1925–1944.

Menciassi, A., A. Eisinberg, M. C. Carrozza, and P. Dario (2003). Force sensing microinstrument for measuring tissue properties and pulse in microsurgery. *IEEE/ASME Transactions on Mechatronics 8*(1), 10–17.

Miyamoto, Y., W. Kaysser, B. Rabin, A. Kawasaki, and R. Ford (1999). *Functionally Graded Materials: Design, Processing and Applications*. Dordrecht: Kluwer Academic Publishers.

Naillon, M., R. H. Coursant, and F. Besnier (1983). Analysis of piezoelectric structures by a finite element method. *Acta Eletronica 25(4)*, 341–362.

Nishiwaki, S., S. Min, J. Yoo, and N. Kikuchi (2001). Optimal structural design considering flexibility. *Computer Methods in Applied Mechanics and Engineering 190*, 4457–4504.

Paulino, G. and E. Silva (2005). Design of functionally graded structures using topology optimization. *Materials Science Forum 492–493*, 435–440.

Pérez, R., J. Agnus, C. Clévy, A. Hubert, and N. Chaillet (2005). Modeling, fabrication, and validation of a high-performance 2-dof piezoactuator for micromanipulation. *IEEE/ASME Transactions on Mechatronics 10*(2), 161–171.

Rahmatalla, S. and C. C. Swan (2004). A q4/q4 continuum structural topology optimization implementation. *Structural and Multidisciplinary Optimization 27*, 130–135.

Rai-Choudhury, P. (2000). *MEMS and MOEMS Technology and Applications*. Bellingham, Washington, EUA: SPIE Press.

Reynaerts, D., J. Peirs, and H. V. Brussel (1998). A mechatronic approach to microsystem design. *IEEE/ASME Transactions on Mechatronics 3*(1), 24–33.

Sigmund, O. (2000). Topology optimization: a tool for the tailoring of structures and materials. *A special issue of the Philosophical Transactions of the Royal Society: Science into the next Millenium (Issue III, Mathematics, Physics and Engineering 358*(1765), 211–227.

Silva, E. C. N. and N. Kikuchi (1999). Design of piezoelectric transducers using topology optimization. *Journal of Smart Materials and Structures 8*, 350–364.

Silva, E. C. N., S. Nishiwaki, J. S. O. Fonseca, and N. Kikuchi (1999). Optimization methods applied to material and flextensional actuator design using the homogenization method. *Computer Methods in Applied Mechanics and Engineering 172*, 241–271.

Silva, E. C. N., S. Nishiwaki, and N. Kikuchi (2000). Topology optimization design of flextensional actuators. *IEEE Transactions on Ultrasonics, Ferroelectrics and Frequency Control 47*(3), 657–671.

Stolpe, M. and K. Svanberg (2001). On the trajectories of penalization methods for topology optimization. *Structural and Multidisciplinary Optimization 21*, 128–139.

Suresh, S. and A. Mortensen (1988). *Fundamentals of Functionally Graded Materials*. London, England: IOM Communications Ltd.

Turteltaub, S. (2002a). Functionally graded materials for prescribed field evolution. *Computer Methods in Applied Mechanics and Engineering 191*, 2283–2296.

Turteltaub, S. (2002b). Optimal control and optimization of functionally graded materials for thermomechanical processes. *International Journal of Solids and Structures 39*, 3175–3197.

Vanderplaatz, G. N. (1984). *Numerical Optimization Techniques for Engineering Design: with Applications*. New York, USA: McGraw-Hill.

Zhifei, S. (2002). General solution of a density functionally gradient piezoelectric cantilever and its applications. *Smart materials and Structures 11*, 122–129.